

University of Nebraska - Lincoln

DigitalCommons@University of Nebraska - Lincoln

Mechanical & Materials Engineering Faculty
Publications

Mechanical & Materials Engineering,
Department of

2017


Effect of Random Ethylene Comonomer on Relaxation of Flow-Induced Precursors in Isotactic Polypropylene

Benjamin Schammé
University of Nebraska-Lincoln

Eric Dargent
Normandie Université

Lucia Fernandez-Ballester
University of Nebraska-Lincoln, lucia.fernandez@unl.edu

Follow this and additional works at: <https://digitalcommons.unl.edu/mechengfacpub>

 Part of the [Mechanics of Materials Commons](#), [Nanoscience and Nanotechnology Commons](#), [Other Engineering Science and Materials Commons](#), and the [Other Mechanical Engineering Commons](#)

Schammé, Benjamin; Dargent, Eric; and Fernandez-Ballester, Lucia, "Effect of Random Ethylene Comonomer on Relaxation of Flow-Induced Precursors in Isotactic Polypropylene" (2017). *Mechanical & Materials Engineering Faculty Publications*. 343.
<https://digitalcommons.unl.edu/mechengfacpub/343>

This Article is brought to you for free and open access by the Mechanical & Materials Engineering, Department of at DigitalCommons@University of Nebraska - Lincoln. It has been accepted for inclusion in Mechanical & Materials Engineering Faculty Publications by an authorized administrator of DigitalCommons@University of Nebraska - Lincoln.

Published in *Macromolecules* 50 (2017), pp 6396–6403

doi 10.1021/acs.macromol.7b01228

Copyright © 2017 American Chemical Society. Used by permission.

Submitted June 9, 2017; revised August 1, 2017; published August 18, 2017.

Supporting Information follows the **References**.

Effect of Random Ethylene Comonomer on Relaxation of Flow-Induced Precursors in Isotactic Polypropylene

Benjamin Schammé,^{1,2} Eric Dargent,²
and Lucia Fernandez-Ballester¹

¹ Department of Mechanical and Materials Engineering and
Nebraska Center for Materials and Nanoscience,
University of Nebraska–Lincoln,
Lincoln, Nebraska 68588, United States

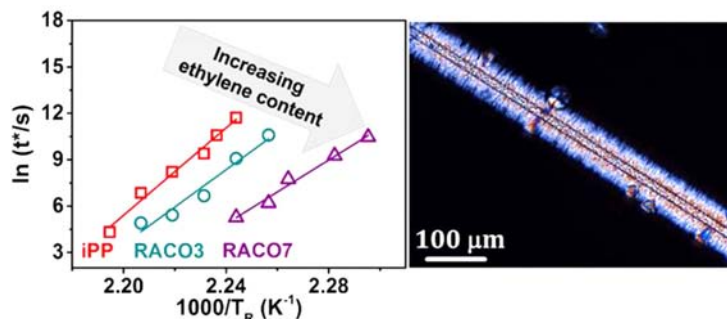
² UNIROUEN Normandie, INSA Rouen, CNRS,
Groupe de Physique des Matériaux,
Normandie Univ., 76000 Rouen, France

Corresponding author — Lucia Fernandez-Ballester, email lucia.fernandez@unl.edu

ORCID: Lucia Fernandez-Ballester: 0000-0001-6956-5104

Abstract

The effect of comonomer on structure and relaxation of flow-induced precursors was investigated in a series of isotactic polypropylene and random propylene–ethylene copolymers. The polymers were subjected to flow by fiber pulling and allowed to relax above their nominal melting temperature for specific times. The type of morphology developed after cooling revealed whether flow-induced precursors were still present or the melt had fully reequilibrated. Precursors were long-lived and, at fixed temperature, decayed significantly faster with higher ethylene content. The critical time for precursor relaxation followed an Arrhenius-type dependence with temperature. The apparent energy of activation for precursor dissolution decreased with increasing comonomer content, indicating that the rate-limiting step of the relaxation process becomes less difficult with higher ethylene fraction. This effect is attributed to ethylene co-units acting as disruptors of precursor structure and is discussed in terms of quasi-crystalline nature and characteristic chain stem length of precursor bundles.



1. Introduction

Imposition of flow onto a polymer melt is well-known to have a tremendous impact on kinetics of crystallization, type of morphology that develops, and, consequently, final material properties. Flow-induced crystallization (FIC) can for instance trigger the formation of highly oriented crystallites and accelerate crystallization kinetics by orders of magnitude, resulting in an increase of the elastic modulus and tensile strength.^{1,2} Most processing techniques of polymers involve the application of strong flows, so understanding the basic mechanism of FIC is key to optimizing the final material properties of a particular resin.

Flow-induced precursors are at the heart of flow-induced crystallization, but they are still not fully understood.^{3–19} FIC oriented precursors are thought to be thread-like quasicrystalline structures that form in the melt during flow and which subsequently template the growth of oriented lamellae, thus dictating the final morphology.^{20,21} The precursors themselves are difficult to probe directly because of their small dimensions and because they are typically present in dilute concentrations, which oftentimes renders them undetectable due to experimental sensitivity limits.^{22,23} Nevertheless, FIC precursors have been detected directly with small-angle X-ray scattering (SAXS) and have also been correlated with an unusual upturn in birefringence during flow.^{10,24} A different approach for studying precursors involves indirect detection: by tracking the development of oriented crystallites which are templated on precursors, the presence of FIC precursors can be inferred. Real-time optical and X-ray measurements as well as ex-situ examination of the final morphology have been used to expose oriented morphologies that indirectly reveal FIC precursors.^{7,9,25,26} Other indirect approaches use rheological measurements or differential scanning calorimetry to follow the increased rates of crystallization associated with flow-induced precursors.^{13,17}

FIC precursors are known to survive for long times at high temperatures even above the nominal melting temperature.⁷ Several studies have investigated the relaxation behavior of flow-induced precursors with the objective of revealing information about their structure and nature. Generally, it has been found that relaxation of FIC precursors follows an Arrhenius-type dependence with an apparent energy of activation that is much larger than the flow activation energy, so the rate-limiting step of relaxation is not controlled by the rheological processes in the melt.^{7-9,13,26-28} A few studies have probed FIC precursors as a function of processing conditions. Balzano et al. found that the imposed shear stress influenced the aspect ratio of oriented precursors of isotactic polypropylene (iPP) which, in turn, determined their stability at high temperatures.¹² Hamad and co-workers observed that FIC precursors created at increasing levels of specific work needed longer annealing times to fully decay.¹³ Furthermore, above certain specific work, the stability of precursors saturated and their response to annealing was independent of flow conditions. Cavallo et al. also reported longer lifetimes for precursors that had formed at higher shear rates, but they established that the rate-determining step of precursor relaxation was unaffected by the level of applied shear rate.⁹ Only a few studies have probed the role of molecular characteristics onto structure and relaxation of FIC precursors. For example, Azzurri et al. found that the relaxation time of precursors of both isotactic polystyrene (iPS) and isotactic polybutene (iPBu) increased with increasing molecular weight M_w ; however, the rate-limiting step for relaxation of precursors did not depend on M_w implying that the structure of precursors was unchanged by differences in length of the polymer chains.^{7,8}

The effect of comonomer content on structure and relaxation of flow-induced precursors of a random polypropylene-ethylene polymer has not previously been explored. Random comonomers can lead to significant changes in the type of crystalline structure that develops, the rates of crystallization, and the final material properties. Specifically, the incorporation of random ethylene co-units onto isotactic polypropylene results in improved impact resistance and mechanical properties at low temperatures as well as increased transparency.²⁹ Random ethylene co-units act as defects and therefore hinder the process of crystallization under quiescent conditions, decreasing rate of crystallite growth, attainable degree of crystallinity, crystallization temperature, and melting temperature.³⁰ Also, the presence of ethylene co-units has been associated with the development of γ -phase in addition to the more common α -morph due to an increased number of short crystallizable sequences.^{30,31} Although early reports assumed that ethylene co-units were fully excluded from the crystal,³² it was later shown that the isotactic polypropylene crystal can include ethylene

defects to certain extent.^{33,34} Flow-induced crystallization of random propylene-co-ethylene can also be affected by the presence of random co-units in the polymer chain, in terms of both formation of FIC precursors and subsequent crystalline growth from the precursors.³⁵

In the current study, the impact of comonomer units on precursor structure and decay for random propylene-ethylene with up to ~7% ethylene is investigated. To do so, precursors are formed by imposing flow via a fiber-pulling protocol; then, the relaxation behavior of the FIC precursors is examined to provide insights into the rate-determining step of their decay and into the structure of the precursors themselves.

2. Experimental Section

2.1. Materials

Three semicrystalline polymers from Borealis were studied: an isotactic polypropylene homopolymer (Borealis HD234CF) and two propylene/ethylene random copolymers (Borealis RD204CF and RD208CF, respectively), synthesized by bulk polymerization in the gas phase using a Ziegler-Natta catalyst.²⁹ Their molecular and physical characteristics have been previously reported in the literature^{29,36} and are summarized in Table 1. Differential scanning calorimetry scans can be found in the Supporting Information. Here, the homopolymer is denoted as "iPP" while the copolymers are denoted as "RACO3" and "RACO7", according to their respective ethylene content of 3.4 and 7.3 mol %. All three grades possess a weight-average molecular weight M_w of 310 kg/mol and a polydispersity index M_w/M_n of 3.4.

Glass-coated fibers Flexstrand 110EM13347 with diameter of 17 ± 1 μm were kindly provided by Fiber Glass Industries and used as received. The fibers were examined with a Quanta 200 FEG environmental scanning electron microscope and were found to have a smooth surface without observable defects or particles. Control crystallization experiments were performed which verified that these glass fibers do not induce preferential crystallization—called transcrystallinity—on the fiber surface under quiescent conditions, i.e., in the absence of flow.

Polypropylene films of approximately 250 μm of thickness were compression molded at 215 °C for 2 min in a Specac hydraulic press and then allowed to slowly cool. Rectangular pieces of 10 mm \times 5 mm were cut from the compression-molded films. To prepare the polymer-fiber composite, a single glass fiber was first carefully extracted from a bundle containing approximately 2000 fibers, and it was inspected to ensure that no bending had occurred. The glass fiber was placed between two ~250 μm thick polymer films. The assembly was then examined to verify that the embedded

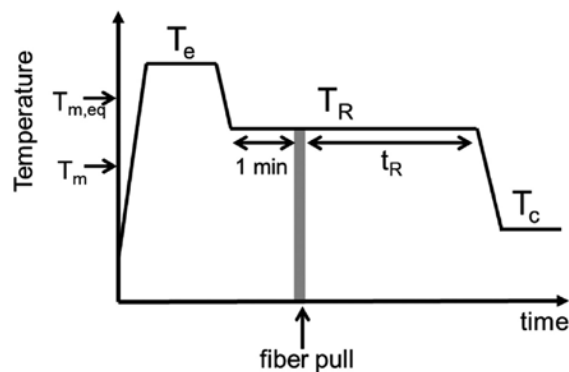


Figure 1. Thermomechanical protocol for relaxation experiments.

fiber was completely straight without any observable curvature. The polymer–fiber composite was subsequently sandwiched between a glass slide and a cover glass which had previously been cleaned with ethanol. The assembly was placed in a Mettler Toledo FP82HT hot stage coupled with a FP90 control system.

2.2. Thermomechanical Protocol

The thermal and flow protocol is schematized in **Figure 1**. First, the assembly was heated to an erase temperature $T_e = 215\text{ °C}$, which is above the equilibrium melting point of iPP ($T_{m,eq} = 208\text{ °C}$).³⁷ A slight pressure was then applied onto the coverslip to ensure that the fiber was well embedded within the polymer and to avoid air bubbles. After pressing, the temperature was held at 215 °C for $t_e = 5\text{ min}$ to erase the previous thermal history of the polymer. Then, the temperature was decreased at a rate of 20 °C/min to the chosen relaxation temperature T_R , which was always selected to be above the nominal melting temperature T_m (**Table 1**). After equilibration at T_R for 1 min , the fiber was manually pulled through the molten polymer at a linear velocity of $5\text{--}10\text{ mm/s}$ over a distance of $5\text{--}10\text{ mm}$. It

Table 1. Molecular and Physical Properties of the Materials from the Literature^{29,36}

<i>polymer</i>	<i>grade</i>	<i>ethylene content (mol %)^a</i>	X_c (%) ^b	T_m (°C) ^b	T_c (°C) ^b
iPP	HD234CF	0	49.5	164	110
RACO3	RD204CF	3.4	41.3	153	105
RACO7	RD208CF	7.3	33.9	139	98

a. Measured by NMR.

b. From differential scanning calorimetry at 10 °C/min .

has previously been found that small differences in pulling velocity or total displacement that may occur when manually pulling the fiber do not appear to affect the results of flow relaxation experiments.⁷ Care was taken to ensure that the movement of the fiber occurred solely in the direction of its axis. After cessation of flow, the sample was allowed to relax at T_R for a specified relaxation time t_R . It should be noted that both flow and relaxation occur at temperatures well above the nominal melting temperature, i.e., at temperatures where lamellar growth rates are negligible.

After the relaxation time t_R had elapsed, the sample was quickly cooled down at 20 °C/min to a suitable crystallization temperature T_c , chosen such that linear growth rates were relatively high and bulk nucleation densities were relatively low (135–138 °C for iPP, 128 °C for RACO3, and 120–122 °C for RACO7). A reference time t_0 was started once T_c was reached. Polarized optical micrographs were obtained every minute up to $t_0 = 30$ min with an Olympus BX51 polarizing optical microscope at 20× magnification. Different areas of the sample were examined in order to account for any possible inhomogeneity in the glass fiber coating. At the end of the experiment, the assembly was removed from the hot stage and air-cooled. The composite was then removed from the slides, and its final thickness was measured.

The axial movement of a fiber in a molten polymer imposes a shear rate $\dot{\gamma}$ with a cylindrical symmetry. Monasse³⁸ showed that the shear rate $\dot{\gamma}$ at a distance r from the fiber axis can be expressed as

$$\dot{\gamma} = \frac{1-n}{n} \frac{1}{r^{1/n}} \left[\frac{1}{r_f^{1-1/n} - r_e^{1-1/n}} \right] V_f \quad (1)$$

where n is the exponent in the viscosity power law equation, r_f is the radius of the glass fiber (8.5 μm), r_e is the external radius (half thickness of the polymer film), r is the radius, and V_f is the velocity of pulling. According to Eq. 1, the shear rate under our flow conditions reaches values in the order of several hundreds of s^{-1} near the surface of the fiber.

3. Results

3.1. Flow-Induced Crystallization Morphology

Imposition of flow by axial movement of a glass fiber embedded in an iPP matrix can result in subsequent growth of a shear-induced oriented morphology near the fiber surface (**Figure 2b**). This oriented structure is not caused by transcrystallinity effects on the fiber surface: control quiescent experiments—in which no flow is applied—developed only a bulk spherulitic morphology throughout the polymer, and there was no preferential

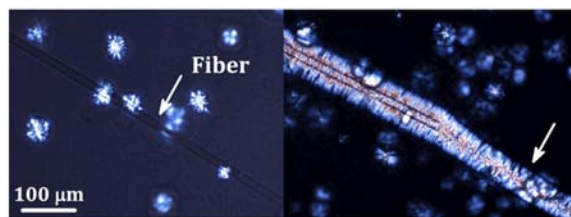


Figure 2. (a) Spherulitic morphology formed after 15 min at $T_c = 135$ °C in a quiescent experiment where no flow has been imposed. (b) Cylindritic morphology formed after 15 min at $T_c = 135$ °C in a shear experiment where the glass fiber was pulled ($T_R = 172.5$ °C, $t_R = 40$ min).

crystalline growth on the fiber surface (Figure 2a). In contrast, a cylindritic oriented morphology can develop in experiments where the fiber has been pulled due to the shear flow imposed by the moving fiber (Figure 2b). The highly oriented structures can also be observed in the wake of the fiber (white arrow in Figure 2b), further confirming that they were not due to transcrystallinity on the fiber surface.^{27,39} When shear flow resulted in oriented crystallization, development of oriented crystallites only took place close to the fiber surface, where the highest levels of shear rate occurred. Further from the fiber surface, only spherulites typical of quiescent conditions were obtained due to the rapid decrease of shear rate with distance from the fiber. Both the cylindritic and the spherulitic structures developed with identical linear growth rate G , indicating that lamellar growth rate is not affected by the previous flow history.⁷

In shear experiments, a small birefringent zone around the fiber was briefly observed while the fiber was being pulled and can be attributed to increased orientation of polymer chains while subjected to high shear rates. Even though that melt birefringence quickly disappears after cessation of flow, the effects of shear on final morphology can persist for very long times, in agreement with other studies. For example, iPP still retains some orientation after a relaxation time of ~ 15 min at 180 °C and of ~ 3 h at 175 °C (see Relaxation Experiments section). Long-lived effects of flow have also been reported by other authors, such as relaxation times between 1 and 32 min at 190 °C.^{9,26,28,40,41} In other words, the conformation of polymer chains in the melt is distorted by the imposition of flow, and such distortion can persist for relatively long times, determining the type of semi-crystalline morphology that forms upon cooling down.

3.2. Determination of Critical Holding Time t^*

The growth of a cylindritic morphology around the fiber after cessation of flow is a clear and exceptionally sensitive indicator of remaining perturbation in the polymer melt, i.e., of the presence of flow-induced precursors (FIC precursors). The

development of an oriented morphology implies that even if the sample was allowed to relax for a given relaxation time t_R , complete re-equilibration of the polymer melt was not attained. In contrast, the absence of high nucleation density around the fiber for experiments with large enough relaxation times t_R indicates that the melt was able to fully reach a re-equilibrated state.

To quantify the melt re-equilibration process, a critical relaxation time t^* is defined as the holding time necessary to completely erase the effect of the applied flow. Here, t^* at each relaxation temperature T_R is calculated as the average of two values: the maximum relaxation time t_{MAX}^* for which some preferential nucleation on the fiber surface is still observed upon cooling to T_c and the minimum relaxation time t_{MIN}^* for which only a spherulitic morphology is detected.

Increasing the relaxation time t_R at a fixed relaxation temperature T_R generally resulted in a decline of nucleation density near the fiber. For example, increasing t_R from 5 s to 15 min at $T_R = 180$ °C resulted in a partial disappearance of flow-induced precursors, as inferred from the observed morphologies (**Figure 3a–c**). Once t_R exceeded the critical time t^* , the melt memory due to flow was fully erased and only spherulites developed throughout (i.e., $t_R = 20$ min in **Figure 3d**).

3.3. Relaxation Experiments

The critical holding time t^* was determined at different relaxation temperatures T_R by examining the final morphology that appeared after allowing

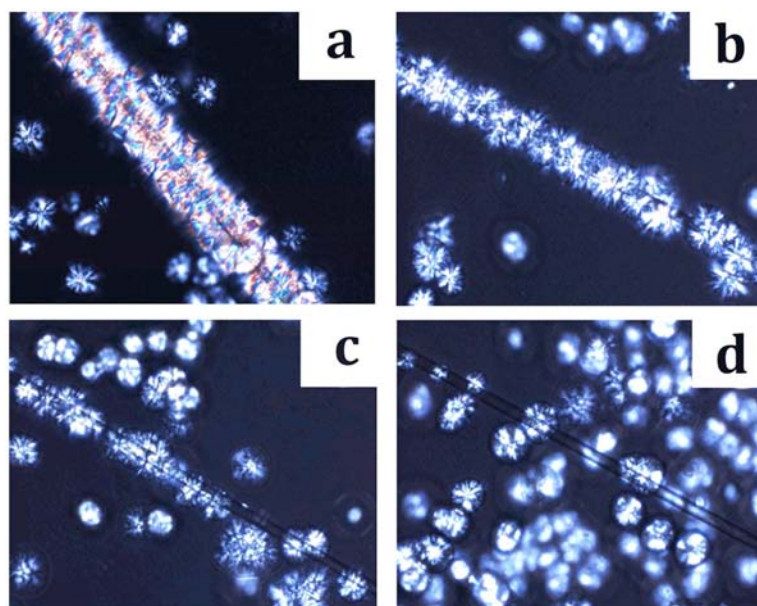


Figure 3. Morphological evolution of iPP after 15 min at $T_c = 135$ °C in fiber pull experiments with $T_R = 180$ °C and relaxation times t_R of (a) 5 s, (b) 10 min, (c) 15 min, and (d) 20 min.

relaxation to occur for a specific relaxation time t_R and then cooling to a suitable crystallization temperature T_C . In this way, the morphological outcome of each fiber pull experiment was classified to construct a morphological map for each type of material. Selection criteria were based on Figure 3: extensive cylindrical morphology was denominated “high orientation” (Figure 3a,b), decreased nucleation along the fiber—but still preferential—was regarded as “low orientation” (Figure 3c), and the presence of only bulk spherulitic morphology was denominated “spherulitic” (Figure 3d). It should be noted that the distinction between high and low orientation was qualitative only. The morphological map of iPP is shown in **Figure 4**, while those of RACO3 and RACO7 can be found in the Supporting Information. The dashed line in Figure 4 represents the critical time t^* calculated as the average between the maximum holding time t_{MAX}^* for observing some cylindrical morphology and the minimum time t_{MIN}^* for which only a spherulitic morphology is obtained. The values for t_{MAX}^* and t_{MIN}^* at different relaxation temperatures T_R for all three materials are reported in **Table 2**.

For a given material, the strong temperature dependence of the critical times t^* (dashed line in Figure 4) indicates that the lifetime of flow-induced precursors is a highly sensitive function of relaxation temperature T_R . As an example, the time required to fully erase the shear-induced nucleation for iPP increases from ~16 min at 180 °C to more than 30 h at 172.5 °C. Such strong temperature dependence is consistent with previous studies; for example, work on poly(1-butene) found that the critical time increased by 3 orders of magnitude when the relaxation temperature was decreased by 10 °C.⁷

For a given relaxation temperature T_R , the critical time for disappearance of the oriented morphology t^* significantly decreases with increasing comonomer content. For example, at 172.5 °C, iPP needs more than 30 h to

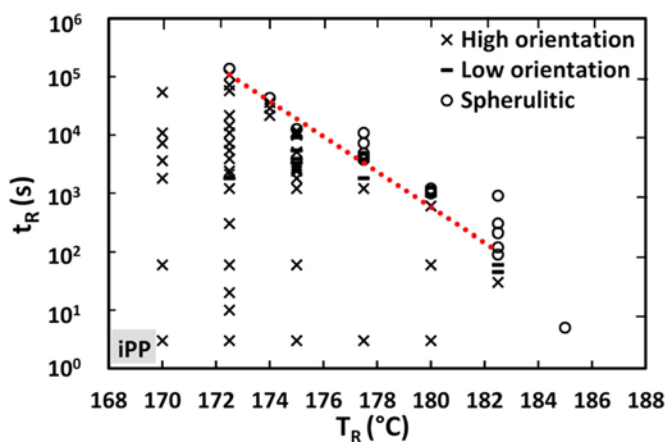


Figure 4. iPP morphological map for relaxation experiments. Dashed line corresponds to a linear fit of the calculated critical relaxation times t^* .

Table 2. Critical Holding Times t^* at Different T_R for iPP, RACO3, and RACO7^a

T_R (°C)	t^* (s)		
	iPP	RACO3	RACO7
182.5	60–90		
180	900–990	120–150	
177.5	3600–3750	210–240	
175	11700–12600	750–810	
174	36000–43200		
172.5	108000–136800	8520–9000	180–210
170		36000–43200	480–510
168.5			2250–2325
165			10320–10800
162.5			30600–39600

a. The first and second value in each pair correspond to t_{M}^{*AX} (maximum time for some cylindrical morphology) and t_{M}^{*IN} (minimum time for only spherulitic morphology), respectively.

completely relax the oriented morphology, while RACO3 and RACO7 only need ~2.5 h and 3.5 min, respectively (Table 2). Likewise, with increasing ethylene content, the temperature of relaxation T_R needs to be lowered in order to obtain similar values of critical relaxation time t^* . It was also found that the highest temperature T_R for which oriented crystallization could be obtained—using the shortest possible holding times—decreases with increasing comonomer content. Indeed, it was not possible to obtain cylindrical structures after fiber pulling for T_R above 182.5, 180, and 172.5 °C for iPP, RACO3, and RACO7, respectively. Such a threshold on T_R may have been caused in part by limitations in cooling speed: at the highest relaxation temperatures where t^* is on the order of ~5 s or smaller, the experimental setup cannot be cooled fast enough to prevent some relaxation of flow-induced structures during the early stages of cooling. Additionally, it is possible that flow-induced structures are not able to form at the highest temperatures if crystallizable sequences are not long enough, particularly as the comonomer content increases.

The apparent activation energy E_a for complete disappearance of flow-induced structures was found to decrease with increasing copolymer content. To calculate E_a , the average critical time t^* was first plotted against the inverse of temperature in an Arrhenius plot (**Figure 5**). A set of straight lines was obtained, so Eq. 2 was used to obtain values of E_a for each material:

$$\ln(t^*) = \ln(A) - \frac{E_a}{R} \left(\frac{1}{T} \right) \quad (2)$$

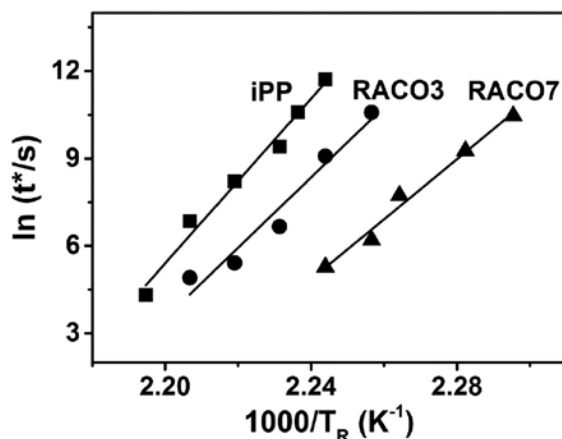


Figure 5. Arrhenius plot of critical holding times t^* as a function of relaxation temperature T_R for iPP (■), RACO3 (●), and RACO7 (▲).

where t^* (in s) is the critical relaxation time, A is a preexponential factor, R is the gas constant ($8.314 \text{ J K}^{-1} \text{ mol}^{-1}$), and T is the absolute temperature (in K). Energies of activation of 1180 ± 60 , 1000 ± 50 , and $860 \pm 40 \text{ kJ/mol}$ were obtained for iPP, RACO3, and RACO7, respectively.

4. Discussion

The development of an oriented morphology near the fiber surface is an extremely sensitive indicator of the presence of oriented precursors that formed during strong enough flows. These oriented precursors are thought to be crystalline or quasi-crystalline thread-like nuclei, although their exact structure remains the subject of discussion. In the present experiments, flow-induced precursors form during flow in the region subjected to the highest level of shear stress—near the fiber surface. After cessation of flow, the oriented precursors can undergo a gradual disappearance process if the polymer melt is held at sufficiently high relaxation temperature for a long time. The dissolution of precursors is reflected in a decrease in oriented morphologies developed after cooling to the crystallization temperature.

The Arrhenius-type dependence with temperature of the critical times for relaxation provides some insight into the manner in which oriented precursors decay. The process of flow-induced precursor relaxation is believed to occur by detachment of polymer chain segments from the oriented nuclei and their subsequent diffusion into the melt. The apparent energies of activation for precursor relaxation of iPP, RACO3, and RACO7 are much larger than the energy of activation for viscous flow ($\sim 44 \text{ kJ/mol}$ for iPP).⁴² Therefore, it appears that detachment of a chain stem from an oriented

nuclei is the limiting step in the process of precursor relaxation—not diffusion of the detached stem into the melt. This observation is in agreement with studies of relaxation in iPP, iPS, and iPBu.^{7,9,26}

The decrease of apparent activation energies E_a with increasing ethylene content indicates that the rate of the relaxation process is altered by the presence of comonomer. This may be attributed to the disruption of the structure of oriented precursors and thus to the process of chain stem detachment from quasi-crystalline precursor bundles. It is well-known that random ethylene co-units in polypropylene play a major role by acting as perturbations of the resulting crystalline structure, so the reduction of E_a with increasing ethylene content suggests that those random co-units are also effective at perturbing the morphological nature of the precursors.

The apparent activation energies E_a can be used to obtain information about the structure of flow-induced precursors, which have been proposed to consist of partially ordered bundles of chains with a quasi-crystalline nature and a characteristic bundle length L_s .⁸ In this model, it is envisioned that precursors decay by having chain segments of length L_s disengage from the precursor bundles. The length L_s may then be determined as

$$L_s = \frac{E_a}{\Delta H_m^0} \times L_u \quad (3)$$

where L_u corresponds to the length of the repeating unit along the c -axis in the crystalline lattice, E_a is the apparent activation energy for disappearance of oriented precursors, and ΔH_m^0 is the melting enthalpy of the polymer crystals. For iPP, L_u is ~ 0.22 nm⁴³ and the thermodynamic melting enthalpy of its crystals ΔH_m^0 is 8.7 kJ/mol.⁴⁴ However, if the melting enthalpy of a perfect iPP crystal is used in calculations for random copolymers, their detaching chain length L_s may be underestimated. Indeed, random ethylene co-units are known to be partially included into the crystalline phase of iPP, locally distorting it and resulting in a decrease of the energy required to melt it.^{34,45} Consequently, the melting enthalpies of copolymer crystallites are projected to be lower than 8.7 kJ/mol.

For random copolymers, the exact dependence of the melting enthalpy of the crystalline phase with the fraction of incorporated comonomer units is unknown. One approach for obtaining an estimate of the melting enthalpy is to use the Sanchez–Eby theory of copolymers, which considers an excess free energy ϵ associated with comonomers incorporated into the crystalline phase as defects.⁴⁶ Although the variation of the melting enthalpy with ϵ remains elusive, some authors have assumed a linear dependency $\Delta H_{\text{cryst,cop}} = \Delta H_{\text{cryst,homo}} - \epsilon X_c$, where $\Delta H_{\text{cryst,cop}}$ is the heat of fusion per mole of crystalline copolymer, $\Delta H_{\text{cryst,homo}}$ is the heat of fusion per mole of crystalline homopolymer (8.7 kJ/mol), and X_c is the mole fraction

of ethylene co-units in the crystalline phase of the copolymer.^{47,48} For polypropylene–ethylene copolymers, Alamo et al. experimentally obtained data for X_c and calculated a penalty energy ϵ of ~ 2.94 kJ/mol.^{34,47} Using these literature values, it is estimated that the $\Delta H_{\text{cryst,RACO7}}$ would only decrease by $\sim 0.9\%$ when compared to 8.7 kJ/mol of the iPP homopolymer, indicating that the ethylene counts only slightly distort the energy landscape of the crystalline structure. The corresponding detaching stem lengths L_s are 30, 25, and 22 nm for iPP, RACO3, and RACO7, respectively (**Table 3**).

Another approach to estimate the melting enthalpy of 100% crystalline phase $\Delta H_{\text{cryst,cop}}$ involves measuring the experimental heat of fusion of a given sample with differential scanning calorimetry and then determining its crystallinity with an alternative experimental technique. Laihonen et al. normalized the experimental heat of fusion by the crystallinity obtained from wide-angle X-ray diffraction and determined that $\Delta H_{\text{cryst,cop}}$ decreased by $\sim 30\text{--}40$ J/g per 10% of ethylene content.⁴⁹ Using Laihonen's result, a $\Delta H_{\text{cryst,RACO7}}$ of ~ 7.7 kJ/mol can be estimated for RACO7, i.e., a steeper decrease than that calculated with ϵ . The resulting values of L_s still show a decrease with increasing copolymer percentage: 30, 27, and 24 nm for iPP, RACO3, and RACO7 (Table 3). Finally, in another study, Alamo et al. also obtained measurements of experimental enthalpy of fusion and corresponding NMR crystallinities for a series of polypropylene–ethylene copolymers.³⁴ If the experimental melting enthalpies are normalized by their corresponding ^{13}C NMR crystallinities, an even stronger decrease in enthalpy with ethylene content is predicted: for RACO7, $\Delta H_{\text{cryst,RACO7}}$ would be ~ 6.6 kJ/mol. In this case, however, the obtained detaching stem lengths L_s display an almost constant value of approximately 30 nm (Table 3).

While the decrease in E_a indicates that the process of chain stem detachment from quasi-crystalline bundles becomes less difficult with increasing ethylene content, the exact interpretation in terms of structural parameters of precursors is complicated by the uncertainty in $\Delta H_{\text{cryst,cop}}$. The values of L_s obtained with ϵ and with Laihonen's data suggest that ethylene counts mainly disrupt structure of precursors by decreasing the

Table 3. Values of Apparent Energy of Activation for Precursor Relaxation E_a and Stem Length L_s Calculated with $\Delta H_{\text{cryst,cop}}$ Estimated Using Excess Free Energy ϵ , a Decrease of 30–40 J/g per 10 mol % Ethylene,⁴⁹ and Data on Heat of Fusion and on ^{13}C NMR Crystallinities³⁴ (further details are available in the Supporting Information).

sample	E_a (kJ/mol)	$L_{s,\text{excess free energy}}$ (nm)	$L_{s,\text{Laihonen}}$ (nm) ⁴⁹	$L_{s,\text{Alamo}}$ (nm) ³⁴
iPP	1180	30	30	30
RACO3	1000	25	27	30
RACO7	860	22	25	29

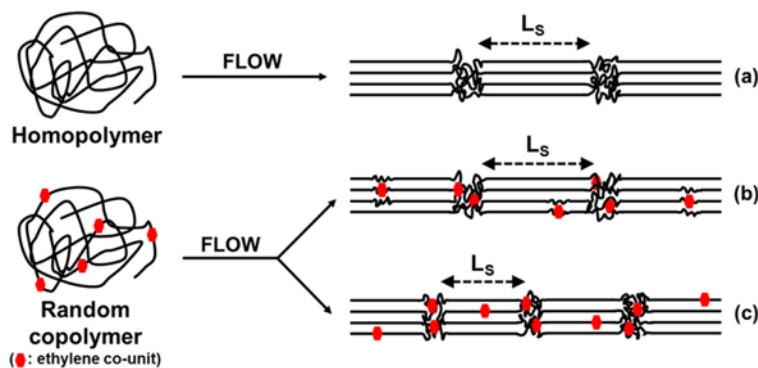


Figure 6. Schematic of flow-induced precursors of (a) a homopolymer and (b, c) a copolymer. (a) The homopolymer forms precursors with a characteristic detaching stem length L_s . (b) The copolymer forms precursors with L_s similar to that of the homopolymer if its counts predominantly increase the degree of imperfection within the internal structure of bundles (decrease in $\Delta H_{\text{cryst,cop}}$). (c) The copolymer forms precursors with decreased L_s if the presence of comonomer mainly decreases the average length of precursor bundles ($\Delta H_{\text{cryst,cop}}$ nearly invariant).

average length of precursor bundles—and thus, the length of chain stem L_s that must detach during decay (schematically illustrated in **Figure 6**, compare a and c). In contrast, L_s determined by normalizing with ^{13}C NMR crystallinities suggests that ethylene comonomers predominantly disturb precursor structure by increasing the internal degree of imperfection of quasi-crystalline bundles (Figure 6, compare a and b). This divergence may be due to the fact that ^{13}C NMR crystallinity considers the fraction of ordered 3/1 helical sites (crystallites) but does not take into account how perfectly packed those helices are.³⁴ Imperfections in packing of helices can result in decreased calorimetry or wide-angle X-ray diffraction crystallinities without significantly changing the magnitude of NMR crystallinity, yielding differing estimates of $\Delta H_{\text{cryst,cop}}$ (and L_s) depending on which experimental technique is used.

Because of the uncertainty in melting enthalpy of copolymer crystals, it is not possible to discern between the effect of comonomer units on precursors as depicted in Figure 6b,c. Also, qualitative arguments can be made for both possible scenarios. On one hand, if the characteristic lamellar thickness of a polymer is considered to be related to precursor stem length L_s , a reduction in L_s with increasing coethylene content—as estimated from calculations based on Sanchez–Eby and Laihonon (Table 3)—would be expected. Indeed, lamellar thickness in polypropylene–ethylene random copolymers generally decreases with increasing ethylene percentage,^{29,50–52} although invariance of lamellar thickness with comonomer content has also been reported.³³ The decrease in crystallite thickness

with higher comonomer percentage is generally explained as follows: because a fraction of ethylene units must be excluded from the polypropylene crystals, a resin with higher copolymer content has a smaller average length of crystallizable sequences which can then only participate in lamellae of reduced thickness. On the other hand, it can be hypothesized that due to their quasi-crystalline nature, flow-induced precursors are able to accommodate ethylene counts more easily than a “regular” α -crystal because defects impose less strain on their structure. In other words, the more disordered structure of precursors—as compared to iPP α -phase—would experience less disruption due to inclusion of ethylene defects and would not be as limited by available crystallizable lengths, leading to invariance of L_s with increasing copolymer content as computed from ^{13}C NMR data.

The activation energy E_a and, consequently, the detaching stem length L_s obtained here for iPP are somewhat greater than in previous relaxation experiments of iPP (~ 30 nm vs ~ 7 nm). Notably, an $L_s \sim 30$ nm for iPP is commensurate with the periodicity of layer-like precursors of iPP previously inferred from real-time small-angle X-ray scattering (~ 43 nm)³ and similar to the detaching stem length obtained for relaxation of other types of polymers, namely polyoxyethylene and ipolybutene (~ 20 nm).^{8,27} The value of 30 nm is also comparable to the lamellar thickness of iPP characteristic of relatively high crystallization temperature: under quiescent conditions at 152 °C, a lamellar thickness of ~ 20 nm and corresponding long period of ~ 30 nm would be expected,⁴⁸ while early kebabs grown after flow at low undercoolings can display a long period of up to ~ 60 nm.⁵³ The larger activation energy E_a obtained here for iPP (~ 1180 kJ/mol vs a range of ~ 122 – 350 kJ/mol in other reports)^{9,13,26–28} may be due to differences in experimental protocol. Indeed, discrepancies in E_a are ubiquitous in the literature and have been ascribed to variability in the experimental approach. For example, Janeschitz-Kriegl obtained an $E_a \sim 224$ kJ/mol for iPB,²⁶ about one-third of the value of ~ 720 kJ/mol previously found by Azzurri.⁷ For iPP, Nazari et al. obtained an apparent activation energy of 122 kJ/mol,¹³ much smaller than that of 334 kJ/mol previously reported by Janeschitz-Kriegl.²⁶ These disparities were attributed to using different criteria when determining t^* —assessment of complete disappearance of orientation vs a criterion of partial decay—and to employing different techniques to detect precursors, which can lead to dissimilar definitions of “presence of precursors”. Experimental conditions such as flow geometry, range of shear rate, and range of relaxation temperature also vary widely among different studies, but it is unclear whether sufficiently large variations could generate structural differences in precursors that affect the process of stem detachment and the apparent energy of activation. For example, Cavallo et al. reported that changing shear rate $\dot{\gamma}$ from 16 to 32 s^{-1} does not noticeably affect the

apparent activation energy for relaxation of precursors in iPP (i.e., the rate-determining step for relaxation is independent of shear rate within the explored range), although the critical time for disappearance of the precursors is larger for higher shear rates.⁹ In the current study, fiber pulling can impose shear rates on the order of several hundreds of s^{-1} , but it is undetermined whether such difference in flow conditions would significantly affect precursor structure. Likewise, here precursors have formed in a range of temperatures. However, the role of shearing temperature on the structure of flow-induced precursors has not previously been explored, and consequently, whether it has a significant impact on the rate-limiting step of relaxation remains unknown.

5. Conclusion

The relaxation behavior of flow-induced precursors in iPP provides information about their nature and underlying structure. These oriented precursors are key to the effects of flow-induced crystallization but are extremely difficult to directly probe due to their small size and to their scarce concentration in the melt. In this study, the presence or absence of flow-induced precursors was deduced from the type of semicrystalline morphology that forms near the surface of a previously pulled fiber, i.e., in the region that was subjected to the highest shear rate. The process of decay of precursors was explored by first imposing flow and then allowing the melt to relax at relatively high temperatures T_R for specific relaxation times t_R before cooling down to a crystallization temperature T_C .

It was found that the process of decay of flow-induced precursors is affected by the presence of random ethylene counits in the polypropylene chain. The critical times for precursor relaxation t^* followed an Arrhenius-type dependence with temperature, and the apparent energy of activation for precursor dissolution E_a clearly decreased with increasing ethylene content. Such a decrease indicated that the limiting step in the process of precursors decay is effectively altered by the presence of random comonomer units. E_a values for all three materials were much larger than the activation energy for viscous flow of iPP so, in agreement with other studies, it is deduced that the limiting step in precursor decay is detachment of a chain stem from an oriented nuclei—not diffusion of the detached stem into the melt.

The decrease of apparent activation energy E_a indicates that the process of chain stem detachment becomes easier with increasing ethylene content. This effect is attributed to disruption of the structure of precursors caused by the random ethylene counits. Oriented precursors are envisioned as quasicrystalline bundles from which chain stems of a characteristic length

L_s become detached—with an associated enthalpy—during the relaxation process. The enthalpy of crystallization of polypropylene-*random*-ethylene copolymers $\Delta H_{\text{cryst,cop}}$ is however not well-known, leading to some uncertainty when estimating the detaching stem length L_s . Estimations of $\Delta H_{\text{cryst,cop}}$ based on available experimental data suggest two possible scenarios: one in which ethylene counits mainly disrupt structure of precursors by decreasing the average length of precursor bundles—and therefore the detaching stem length L_s —and another one in which ethylene comonomers primarily disturb precursor structure by increasing the degree of imperfection of the quasi-crystalline bundles.

Acknowledgments — The research was performed in part in the Nebraska Nanoscale Facility: National Nanotechnology Coordinated Infrastructure and the Nebraska Center for Materials and Nanoscience, which are supported by the National Science Foundation under Award ECCS 1542182 and the Nebraska Research Initiative. M. L. Auad is thanked for performing differential scanning calorimetry. The authors declare no competing financial interest.

References

- 1) Kalay, G.; Bevis, M. J. Processing and physical property relationships in injection-molded isotactic polypropylene 0.2. Morphology and crystallinity. *J. Polym. Sci., Part B: Polym. Phys.* 1997, *35* (2), 265–291.
- 2) Schrauwen, B. A. G.; Von Breemen, L. C. A.; Spoelstra, A. B.; Govaert, L. E.; Peters, G. W. M.; Meijer, H. E. H. Structure, deformation, and failure of flow-oriented semicrystalline polymers. *Macromolecules* 2004, *37* (23), 8618–8633.
- 3) Somani, R. H.; Yang, L.; Hsiao, B. S. Precursors of primary nucleation induced by flow in isotactic polypropylene. *Phys. A* 2002, *304* (1–2), 145–157.
- 4) Somani, R. H.; Yang, L.; Hsiao, B. S.; Fruitwala, H. Nature of shear-induced primary nuclei in iPP melt. *J. Macromol. Sci., Part B: Phys.* 2003, *42* (3), 515–531.
- 5) Somani, R. H.; Sics, I.; Hsiao, B. S. Thermal stability of shear-induced precursor structures in isotactic polypropylene by rheo-X-ray techniques with couette flow geometry. *J. Polym. Sci., Part B: Polym. Phys.* 2006, *44* (24), 3553–3570.
- 6) García Gutiérrez, M.-C.; Alfonso, G. C.; Riekkel, C.; Azzurri, F. Spatially Resolved Flow-Induced Crystallization Precursors in Isotactic Polystyrene by Simultaneous Small- and Wide-Angle X-ray Microdiffraction. *Macromolecules* 2004, *37* (2), 478–485.
- 7) Azzurri, F.; Alfonso, G. C. Lifetime of shear-induced crystal nucleation precursors. *Macromolecules* 2005, *38* (5), 1723–1728.
- 8) Azzurri, F.; Alfonso, G. C. Insights into formation and relaxation of shear-induced nucleation precursors in isotactic polystyrene. *Macromolecules* 2008, *41* (4), 1377–1383.

- 9) Cavallo, D.; Azzurri, F.; Balzano, L.; Funari, S. S.; Alfonso, G. C. Flow Memory and Stability of Shear-Induced Nucleation Precursors in Isotactic Polypropylene. *Macromolecules* 2010, *43* (22), 9394–9400.
- 10) Balzano, L.; Kukalyekar, N.; Rastogi, S.; Peters, G. W. M.; Chadwick, J. C. Crystallization and dissolution of flow-induced precursors. *Phys. Rev. Lett.* 2008, *100* (4), 048302.
- 11) Balzano, L. G.; Rastogi, S.; Peters, G. W. M. Crystallization and Precursors during Fast Short-Term Shear. *Macromolecules* 2009, *42* (6), 2088–2092.
- 12) Balzano, L.; Cavallo, D.; Van Erp, T. B.; Ma, Z.; Housmans, J.-W.; Fernandez-Ballester, L.; Peters, G. W. M. Dynamics of fibrillar precursors of shishes as a function of stress. *IOP Conf. Ser.: Mater. Sci. Eng.* 2010, *14* (1), 012005.
- 13) Hamad, F. G.; Colby, R. H.; Milner, S. T. Lifetime of Flow-Induced Precursors in Isotactic Polypropylene. *Macromolecules* 2015, *48* (19), 7286–7299.
- 14) Balzano, L.; Ma, Z.; Cavallo, D.; van Erp, T. B.; Fernandez-Ballester, L.; Peters, G. W. M. Molecular Aspects of the Formation of Shish-Kebab in Isotactic Polypropylene. *Macromolecules* 2016, *49* (10), 3799–3809.
- 15) Liedauer, S.; Eder, G.; Janeschitz-Kriegl, H. On the Limitations of Shear-Induced Crystallization in Polypropylene Melts. *Int. Polym. Process.* 1995, *10* (3), 243–250.
- 16) Kumaraswamy, G.; Kornfield, J. A.; Yeh, F. J.; Hsiao, B. S. Shear-enhanced crystallization in isotactic polypropylene. 3. Evidence for a kinetic pathway to nucleation. *Macromolecules* 2002, *35* (5), 1762–1769.
- 17) Nazari, B.; Rhoades, A. M.; Schaake, R. P.; Colby, R. H. Flow-Induced Crystallization of PEEK: Isothermal Crystallization Kinetics and Lifetime of Flow-Induced Precursors during Isothermal Annealing. *ACS Macro Lett.* 2016, *5* (7), 849–853.
- 18) Zhao, Y.; Hayasaka, K.; Matsuba, G.; Ito, H. In Situ Observations of Flow-Induced Precursors during Shear Flow. *Macromolecules* 2013, *46* (1), 172–178.
- 19) An, H.; Li, X.; Geng, Y.; Wang, Y.; Wang, X.; Li, L.; Li, Z.; Yang, C. Shear-Induced Conformational Ordering, Relaxation, and Crystallization of Isotactic Polypropylene. *J. Phys. Chem. B* 2008, *112* (39), 12256–12262.
- 20) Liedauer, S.; Eder, G.; Janeschitz-Kriegl, H.; Jerschow, P.; Geymayer, W.; Ingolic, E. On the Kinetics of Shear-Induced Crystallization in Polypropylene. *Int. Polym. Process.* 1993, *8* (3), 236–244.
- 21) Kumaraswamy, G.; Verma, R. K.; Issaian, A. M.; Wang, P.; Kornfield, J. A.; Yeh, F.; Hsiao, B. S.; Olley, R. H. Shear-enhanced crystallization in isotactic polypropylene Part 2. Analysis of the formation of the oriented “skin”. *Polymer* 2000, *41* (25), 8931–8940.
- 22) Fernandez-Ballester, L.; Gough, T.; Meneau, F.; Bras, W.; Ania, F.; Francisco, J. C.; Kornfield, J. A. Simultaneous birefringence, small-angle wide-angle X-ray scattering to detect precursors and characterize morphology development during flow-induced crystallization of polymers. *J. Synchrotron Radiat.* 2008, *15*, 185–190.
- 23) Ma, Z.; Balzano, L.; Peters, G. W. M. Dissolution and Reemergence of Flow-Induced Shish in Polyethylene with a Broad Molecular Weight Distribution. *Macromolecules* 2016, *49* (7), 2724–2730.

- 24) Kumaraswamy, G.; Issaian, A. M.; Kornfield, J. A. Shear-enhanced crystallization in isotactic polypropylene. 1. Correspondence between in situ rheo-optics and ex situ structure determination. *Macromolecules* 1999, 32 (22), 7537–7547.
- 25) Fernandez-Ballester, L.; Thurman, D. W.; Kornfield, J. A. Realtime depth sectioning: Isolating the effect of stress on structure development in pressure-driven flow. *J. Rheol.* 2009, 53 (5), 1229–1254.
- 26) Janeschitz-Kriegl, H.; Eder, G. Shear Induced Crystallization, a Relaxation Phenomenon in Polymer Melts: A Re-Collection. *J. Macromol. Sci., Part B: Phys.* 2007, 46 (3), 591–601.
- 27) Alfonso, G. C.; Scardigli, P. Melt memory effects in polymer crystallization. *Macromol. Symp.* 1997, 118, 323–328.
- 28) Isayev, A. I.; Chan, T. W.; Shimojo, K.; Gmerek, M. Injection-Molding of Semicrystalline Polymers 0.1. Material Characterization. *J. Appl. Polym. Sci.* 1995, 55 (5), 807–819.
- 29) Gahleitner, M.; Jaaskelainen, P.; Ratajski, E.; Paulik, C.; Reussner, J.; Wolfschwenger, J.; Neissl, W. Propylene-ethylene random copolymers: Comonomer effects on crystallinity and application properties. *J. Appl. Polym. Sci.* 2005, 95 (5), 1073–1081.
- 30) Jeon, K.; Chiari, Y. L.; Alamo, R. G. Maximum Rate of Crystallization and Morphology of Random Propylene Ethylene Copolymers as a Function of Comonomer Content up to 21 mol %. *Macromolecules* 2008, 41 (1), 95–108.
- 31) Gahleitner, M.; Wolfschwenger, J.; Fiebig, J.; Neissl, W. Influence of nucleants on the formation of shear-induced structures in polypropylene. *Macromol. Symp.* 2002, 185, 77–87.
- 32) Zimmermann, H. J.; Hoehst, A. G. Structural analysis of random propylene-ethylene copolymers. *J. Macromol. Sci., Part B: Phys.* 1993, 32 (2), 141–161.
- 33) Laihonon, S.; Gedde, U. W.; Werner, P. E.; Westdahl, M.; Jääskeläinen, P.; Martinez-Salazar, J. Crystal structure and morphology of melt-crystallized poly(propylene-stat-ethylene) fractions. *Polymer* 1997, 38 (2), 371–377.
- 34) Alamo, R. G.; VanderHart, D. L.; Nyden, M. R.; Mandelkern, L. Morphological Partitioning of Ethylene Defects in Random Propylene–Ethylene Copolymers. *Macromolecules* 2000, 33 (16), 6094–6105.
- 35) Ma, Z.; Fernandez-Ballester, L.; Cavallo, D.; Gough, T.; Peters, G. W. M. High-Stress Shear-Induced Crystallization in Isotactic Polypropylene and Propylene/Ethylene Random Copolymers. *Macromolecules* 2013, 46 (7), 2671–2680.
- 36) Housmans, J.-W.; Peters, G. W. M.; Meijer, H. E. H. Flow-induced crystallization of propylene/ethylene random copolymers. *J. Therm. Anal. Calorim.* 2009, 98 (3), 693.
- 37) Fatou, J. G. Melting temperature and enthalpy of isotactic polypropylene. *Eur. Polym. J.* 1971, 7 (8), 1057–1064.
- 38) Monasse, B. Polypropylene nucleation on a glass fibre after melt shearing. *J. Mater. Sci.* 1992, 27 (22), 6047–6052.
- 39) Monasse, B. Nucleation and anisotropic crystalline growth of polyethylene under shear. *J. Mater. Sci.* 1995, 30 (19), 5002–5012.

- 40) Eder, G.; Janeschitz-Kriegl, H. Crystallization. In *Processing of Polymers*; Meijer, H. E. H., Ed.; Wiley-VCH: New York, 1997; Vol. 18, pp 269–342.
- 41) Stadlbauer, M.; Janeschitz-Kriegl, H.; Eder, G.; Ratajski, E. New extensional rheometer for creep flow at high tensile stress. Part II. Flow induced nucleation for the crystallization of iPP. *J. Rheol.* 2004, 48 (3), 631–639.
- 42) Van Krevelen, D. W. *Properties of Polymers*; Elsevier: Amsterdam, 1990.
- 43) Alexander, L. B. E.; Chalmers, B.; Kurmhansl, J. *X-ray Diffraction Methods in Polymer Science*; Wiley-Interscience: 1969.
- 44) Van Krevelen, D. W.; Te Nijenhuis, K. *Properties of Polymers: Their Correlation with Chemical Structure; Their Numerical Estimation and Prediction from Additive Group Contributions*; Elsevier: 2009.
- 45) De Rosa, C.; Auriemma, F.; de Ballesteros, O. R.; Resconi, L.; Camurati, I. Crystallization Behavior of Isotactic Propylene–Ethylene and Propylene–Butene Copolymers: Effect of Comonomers versus Stereodefects on Crystallization Properties of Isotactic Polypropylene. *Macromolecules* 2007, 40 (18), 6600–6616.
- 46) Sanchez, I. C.; Eby, R. K. Thermodynamics and Crystallization of Random Copolymers. *Macromolecules* 1975, 8 (5), 638–641.
- 47) Alamo, R. G.; Ghosal, A.; Chatterjee, J.; Thompson, K. L. Linear growth rates of random propylene ethylene copolymers. The changeover from γ dominated growth to mixed ($\alpha+\gamma$) polymorphic growth. *Polymer* 2005, 46 (20), 8774–8789.
- 48) Cheng, S. Z. D.; Janimak, J. J.; Zhang, A. Q.; Hsieh, E. T. Isotacticity Effect on Crystallization and Melting in Polypropylene Fractions 0.1. Crystalline-Structures and Thermodynamic Property Changes. *Polymer* 1991, 32 (4), 648–655.
- 49) Laihonon, S.; Gedde, U. W.; Werner, P. E.; Martinez-Salazar, J. Crystallization kinetics and morphology of poly(propylene-statethylene) fractions. *Polymer* 1997, 38 (2), 361–369.
- 50) Hosier, I. L.; Alamo, R. G.; Lin, J. S. Lamellar morphology of random metallocene propylene copolymers studied by atomic force microscopy. *Polymer* 2004, 45 (10), 3441–3455.
- 51) Hosoda, S.; Hori, H.; Yada, K.; Nakahara, S.; Tsuji, M. Degree of comonomer inclusion into lamella crystal for propylene/olefin copolymers. *Polymer* 2002, 43 (26), 7451–7460.
- 52) Mileva, D.; Androsch, R.; Radosch, H.-J. Effect of cooling rate on melt-crystallization of random propylene-ethylene and propylene-1-butene copolymers. *Polym. Bull.* 2008, 61 (5), 643–654.
- 53) Somani, R. H.; Yang, L.; Hsiao, B. S.; Agarwal, P. K.; Fruitwala, H. A.; Tsou, A. H. Shear-induced precursor structures in isotactic polypropylene melt by in-situ rheo-SAXS and rheo-WAXD studies. *Macromolecules* 2002, 35 (24), 9096–9104.

SUPPORTING INFORMATION

Effect of Random Ethylene Comonomer on Relaxation of Flow-Induced Precursors in Isotactic Polypropylene

Benjamin Schammé † §, Eric Dargent §, Lucia Fernandez-Ballester † *

† *Department of Mechanical and Materials Engineering and Nebraska Center for Materials and Nanoscience,, University of Nebraska at Lincoln, Lincoln, Nebraska 68588, United States.*

§ *UNIROUEN Normandie, INSA Rouen, CNRS, Groupe de Physique des Matériaux, Normandie Univ., 76000 Rouen, France*

Morphological maps of RACO3 and RACO7

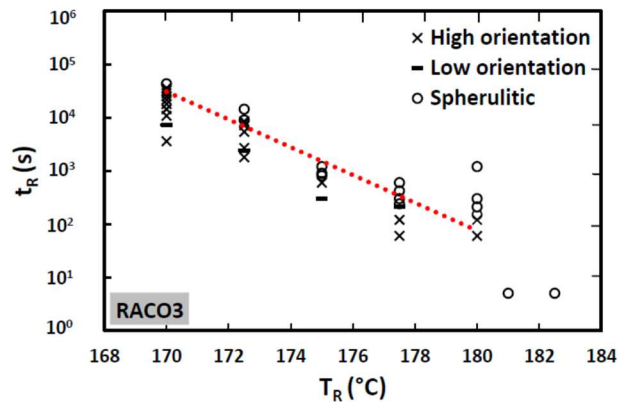


Figure S1. RACO3 morphological map for relaxation experiments. Dashed line corresponds to a linear fit of the calculated critical relaxation times t^* .

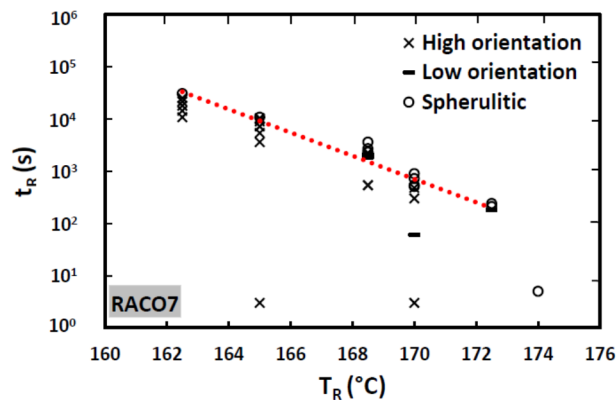


Figure S2. RACO7 morphological map for relaxation experiments. Dashed line corresponds to a linear fit of the calculated critical relaxation times t^* .

Estimation of melting enthalpy of copolymer crystals

The melting enthalpy of copolymer crystals $\Delta H_{\text{cryst,cop},\epsilon}$ estimated using the excess free energy ϵ assumed a linear relationship $\Delta H_{\text{cryst,cop}} = \Delta H_{\text{cryst,homo}} - \epsilon X_c$, where X_c is the mole fraction of ethylene co-units in the crystal. Data for X_c was extracted from a copolymer study by Alamo *et al.*¹, excess free energy $\epsilon \sim 2.94$ kJ/mol was obtained from previous work by the same author,² and 8.7 kJ/mol was used for $\Delta H_{\text{cryst,homo}}$. $\Delta H_{\text{cryst,RACO3}}$ (with 3.4% ethylene) was taken as the average of the values calculated for 2.2% and 4.59%, and $\Delta H_{\text{cryst,RACOy}}$ (with 7.3% ethylene) was taken as that calculated for 7.47% (Table S1).

Ethylene content (mol %)	X_c^1	$\Delta H_{\text{cryst,cop},\epsilon} = \Delta H_{\text{cryst,homo}} - \epsilon X_c$ (kJ/mol)
0.79	0.0035	8.69
2.2	0.0103	8.67
3.4		8.66
4.59	0.0202	8.64
7.47	0.031	8.61

Table S1. Calculations for estimating $\Delta H_{\text{cryst,cop},\epsilon}$.

The melting enthalpy of copolymer crystalline phase $\Delta H_{\text{cryst,cop NMR}}$ was estimated by using ^{13}C NMR crystallinity and experimental heat of fusion (ΔH_{cop}) measured by Alamo *et al.* (Table S2). The enthalpy value for the 0.79% copolymer (considered the homopolymer here) is somewhat smaller than 8.7 kJ/mol (= 209 J/g), so all enthalpy values were normalized to the reference of 8.7 kJ/mol by assessing the relative decrease in enthalpy caused by comonomer (denoted as ratio “r” in Table S2). Note that due to the quasi-crystalline nature of flow-induced precursors, the enthalpy of fusion is in fact expected to be lower (for example, 8.7 kJ/mol would be an overestimation for homopolymer precursors) but the magnitude of that difference is unknown. Thus, in the present work, 8.7 kJ/mol has been used as the reference for the iPP homopolymer.

Ethylene content (mol %)	NMR crystallinity (%) ¹	ΔH_{cop} (J/g)	$\Delta H_{\text{cryst,cop}} = \Delta H_{\text{cop}} / X_c$ (J/g)	$r = \Delta H_{\text{cryst,cop}} / \Delta H_{\text{cryst,0.79\%}}$	$\Delta H_{\text{cryst,cop NMR}} = 8.7 \text{ kJ/mol} * r$ (kJ/mol)
0.79	0.66	92	139.4	1.00	8.7
2.2	0.65	84	129.2	0.93	8.1
3.4					7.4
4.59	0.63	68	107.9	0.77	6.7
7.47	0.58	61	105.2	0.75	6.6

Table S2. Calculations for estimating $\Delta H_{\text{cryst,cop,NMR}}$.

Differential scanning calorimetry

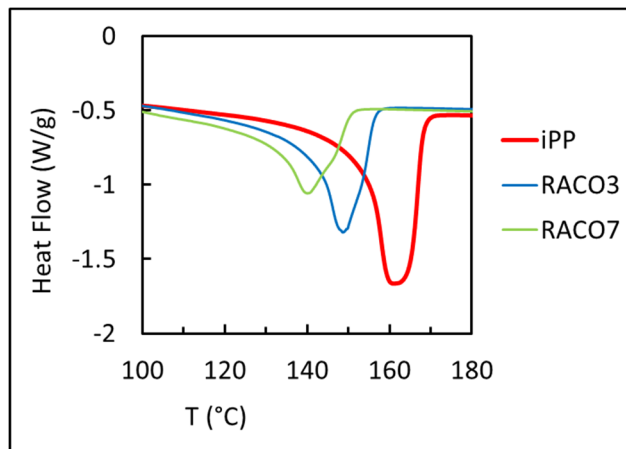


Figure S3. Melting endotherms at a heating rate of 10 °C/min

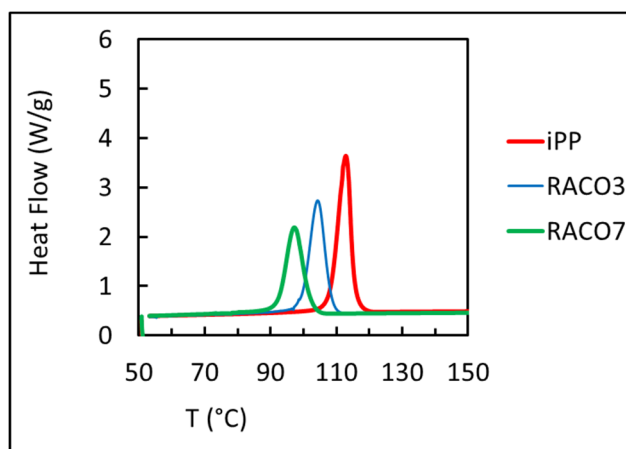


Figure S4. Melting exotherms at a cooling rate of 10 °C/min

References

- ¹ R. G. Alamo, D. L. VanderHart, M. R. Nyden, and L. Mandelkern, *Macromolecules* **33**, 6094 (2000).
- ² R. G. Alamo, A. Ghosal, J. Chatterjee, and K. L. Thompson, *Polymer* **46**, 8774 (2005).